

[DOI] 10.12016/j.issn.2096-1456.202660007

· 基础研究 ·

人骨髓间充质干细胞衰老削弱其衍生凋亡囊泡的骨诱导特性

祝磊, 江雨荷, 张晓

北京大学口腔医学院·口腔医院修复科, 国家口腔医学中心, 口腔疾病国家临床医学研究中心, 口腔生物材料和数字诊疗装备国家工程研究中心, 颅颌面组织生物智造与修复再生北京市重点实验室, 国家卫生健康委口腔数字医学重点实验室, 北京(100081)

【摘要】 目的 探讨亲代人骨髓间充质干细胞(BMSCs)的衰老状态对其衍生凋亡囊泡(apoVs)骨诱导特性的影响,为基于apoVs的牙槽骨缺损及骨质疏松治疗提供实验依据及质量控制参考。方法 本研究通过连续传代构建衰老BMSCs(A-BMSCs)模型,以年轻BMSCs(Y-BMSCs)作为对照。在星形孢菌素诱导细胞凋亡后,分别从Y-BMSCs和A-BMSCs中提取apoVs(Y-BMSCs来源apoVs, Y-apoVs; A-BMSCs来源apoVs, A-apoVs)。首先对2种囊泡的表征(形态、粒径、电位、产量及蛋白标志物等)进行系统鉴定。随后,将Y-BMSCs分为增殖培养(PM)组、成骨诱导(OM)组、OM + Y-apoVs组和OM + A-apoVs组,通过碱性磷酸酶(ALP)染色、茜素红染色及实时定量PCR检测成骨相关基因runt相关转录因子2(RUNX2)、ALP、骨桥蛋白(OPN)及成骨特异性转录因子(OSX)的表达,评估其体外骨诱导效能。获得单位实验动物伦理委员会批准,利用18月龄的C57BL/6老龄小鼠模型验证使用红色荧光染料PKH26标记的2种apoVs的体内分布及骨诱导效能,将小鼠随机分为Control组(注射PBS)、Y-apoVs组(注射Y-apoVs)和A-apoVs组(注射A-apoVs),连续8周尾静脉注射apoVs,通过微计算机断层扫描和组织学分析评估其骨再生效果。结果 电镜及粒径分析显示,Y-apoVs和A-apoVs均呈典型的双凹圆盘状结构,粒径主要分布在100~500 nm;Western blot证实两者均高表达囊泡通用标志物(CD9、CD63、CD81)及凋亡标志物Fas。Y-apoVs和A-apoVs的形态无差异,两者在粒径、电位、产量及蛋白标志物表达差异上均无统计学意义。体外实验显示,与PM组相比,OM组、OM + A-apoVs组、OM + Y-apoVs组均能显著增强靶细胞Y-BMSCs的ALP活性及钙结节沉积,并显著上调RUNX2、ALP、OPN、OSX的表达($P<0.05$);且与OM组及OM + A-apoVs组相比,OM + Y-apoVs组的上述促进作用更为显著($P<0.05$)。体内实验证实,尾静脉注射的apoVs可有效归巢至骨组织,且Y-apoVs组能更有效地改善老龄小鼠的骨微结构,显著提高骨矿物质密度及骨体积分数,其疗效优于Control组和A-apoVs组($P<0.05$)。结论 亲代细胞的衰老状态显著削弱了BMSCs来源apoVs的骨诱导能力。Y-apoVs是治疗年龄相关性骨丢失的有效生物制剂。

【关键词】 骨髓间充质干细胞; 细胞衰老; 细胞外囊泡; 凋亡囊泡; 骨质疏松; 骨再生; 成骨诱导; 无细胞治疗

【中图分类号】 R78 **【文献标志码】** A **【文章编号】** 2096-1456(2026)05-0428-15

【引用著录格式】 祝磊,江雨荷,张晓. 人骨髓间充质干细胞衰老削弱其衍生凋亡囊泡的骨诱导特性[J]. 口腔疾病防治, 2026, 34(5): 428-442. doi:10.12016/j.issn.2096-1456.202660007.

Senescence of human bone marrow mesenchymal stem cells impairs the osteoinductive properties of their derived apoptotic vesicles ZHU Lei, JIANG Yuhe, ZHANG Xiao. Department of Prosthodontics, Peking University School and Hospital of Stomatology & National Center of Stomatology & National Clinical Research Center for Oral Diseases & National Engineering Research Center of Oral Biomaterials and Digital Medical Devices & Beijing Key Laboratory for Intelligent Biomanufacturing and Regeneration of Craniofacial Tissues & NHC Key Laboratory of Digital Stoma-



微信公众号

【收稿日期】 2026-01-04; **【修回日期】** 2026-02-14

【基金项目】 国家自然科学基金项目(82401060); 国家资助博士后研究人员计划(GZC20230138); 北京市自然科学基金项目(7222224)

【作者简介】 祝磊, 博士研究生在读, Email: 18800183672@163.com

【通信作者】 江雨荷, 医师, 博士, Email: jiangyuhe@pku.edu.cn; 张晓, 副教授, 博士, Email: kqxiaozhang@hsc.pku.edu.cn

tology, Beijing, 100081, China

Corresponding author: JIANG Yuhe, Email: jiangyuhe@pku.edu.cn; ZHANG Xiao, Email: kqxiaozhang@hsc.pku.edu.cn

【Abstract】 Objective To investigate the effect of the senescence state of parental human bone marrow mesenchymal stem cells (BMSCs) on the osteoinductive properties of their derived apoptotic vesicles (apoVs), and to provide an experimental basis and a quality control reference for the treatment of alveolar bone defects and osteoporosis based on apoVs. **Methods** A replicative senescence model of human aging BMSCs (A-BMSCs) was established via serial passaging, with young BMSCs (Y-BMSCs) serving as controls. Following the induction of apoptosis with staurosporine, apoVs were isolated from Y-BMSCs and A-BMSCs (termed Y-apoVs and A-apoVs, respectively) via differential centrifugation. The physicochemical properties (morphology, size, zeta potential, and yield) and protein markers of both apoV populations were systematically characterized. Subsequently, Y-BMSCs were divided into a proliferation medium (PM) group, osteogenic induction medium (OM) group, OM + Y-apoVs group, and OM + A-apoVs group. The osteoinductive efficacy *in vitro* was evaluated by alkaline phosphatase (ALP) staining, alizarin red S staining, and quantitative real-time PCR detection of key osteogenic genes, including runt-related transcription factor 2 (RUNX2), ALP, osteopontin (OPN), and osterix (OSX). Approved by the Institutional Animal Care and Use Committee, *in vivo* biodistribution (labelling apoVs with the red fluorescent dye PKH26) and bone regeneration efficacy were assessed in 18-month-old osteoporotic C57BL/6 mice. Mice were randomly divided into a control group (injected with phosphate-buffered saline), Y-apoVs group (injected with Y-apoVs), and A-apoVs group (injected with A-apoVs). Following tail-vein injection administration of apoVs for 8 weeks, bone regeneration was evaluated via micro-computed tomography and histological analysis. **Results** Electron microscopy and particle size analysis revealed that both Y-apoVs and A-apoVs displayed typical biconcave discoid structures, with diameters mainly ranging from 100 to 500 nm. Western blot assays confirmed high expression of universal vesicle markers (CD9, CD63, CD81) and the apoptotic marker Fas in both groups. Y-apoVs and A-apoVs exhibited indistinguishable morphologies, size distributions, zeta potentials, and yields. *In vitro* experiments showed that, compared with the PM group, the OM, OM + A-apoVs, and OM + Y-apoVs groups significantly enhanced ALP activity, calcium nodule formation, and the expression of osteogenic genes (RUNX2, ALP, OPN, OSX) in recipient Y-BMSCs ($P < 0.05$); moreover, compared with the OM and OM + A-apoVs groups, the OM + Y-apoVs group exhibited a more significant promoting effect ($P < 0.05$). An *in vivo* analysis demonstrated that tail-vein-injected apoVs effectively homed to bone tissue. Moreover, the Y-apoVs group significantly improved trabecular microarchitecture, bone mineral density, and bone volume fraction in aged mice, exhibiting superior therapeutic efficacy over the control and A-apoVs groups ($P < 0.05$). **Conclusion** The senescence state of parental cells significantly impairs the osteoinductive ability of BMSC-derived apoVs. Y-apoVs are effective biological agents for the treatment of age-related bone loss.

【Key words】 bone marrow mesenchymal stem cells; cellular senescence; extracellular vesicles; apoptotic vesicles; osteoporosis; bone regeneration; osteoinduction; cell-free therapy

J Prev Treat Stomatol Dis, 2026, 34(5): 428-442.

【Competing interests】 The authors declare no competing interests.

This study was supported by the grants from National Natural Science Foundation of China (No. 82401060); China Postdoctoral Science Foundation (No. GZC20230138) and Beijing Natural Science Foundation (No. 7222224).

随着人口老龄化进程的加速,老年患者的口腔骨缺损修复(如牙周炎导致的牙槽骨吸收、长期缺牙后的牙槽嵴萎缩)已成为口腔临床面临的严峻挑战^[1]。在衰老状态下,骨髓间充质干细胞(bone marrow mesenchymal stem cells, BMSCs)的成骨能力显著下降,限制了自体骨移植及常规骨组织工程的疗效^[2-3]。

近年来,基于细胞外囊泡(extracellular vesicles, EVs)的无细胞疗法因其安全性高、易于储

存和运输等优势,成为口腔再生医学的研究热点^[4]。其中,凋亡囊泡(apoptotic vesicles, apoVs)作为一种特殊的EVs亚群,是细胞在凋亡过程中通过细胞膜起泡和崩解主动释放的纳米级囊泡^[5]。与起源于内体途径的外泌体(exosomes)不同,apoVs不仅产率显著更高(10倍于外泌体)^[6],便于大规模临床级制备^[7],且继承了亲代细胞特异性的核酸与蛋白内容物(如染色质残留、特定的细胞器片段等),在皮肤软组织、肌肉、心血管和骨骼等多种组

织的再生修复和免疫调节中发挥关键作用^[8-12],在调节骨免疫微环境及促进牙槽骨再生方面也展现出独特优势^[13-14]。

然而,目前 apoVs 疗法向临床转化面临的一个核心瓶颈是 apoVs 制剂标准化的缺失^[15]。作为一种生物制剂, apoVs 的治疗效能高度依赖于亲代细胞的生理状态^[16]。BMSCs 具有显著的供体异质性,供体年龄及其体外传代过程中的衰老状态是否会通过 apoVs 传递负面信号,进而影响其修复效能,目前尚不明确^[17]。若衰老 BMSCs (aging BMSCs, A-BMSCs) 来源的 apoVs 治疗效果受损,那么在建立临床级 apoVs 库时,确立严格的供体筛选标准和传代代次限制就显得尤为关键。

因此,本研究拟通过连续传代构建体外 BMSCs 复制性衰老模型,模拟细胞扩增过程中的衰老现象,系统比较年轻 BMSCs (young BMSCs, Y-BMSCs) 来源 apoVs 与 A-BMSCs 来源 apoVs 在物理表征及骨诱导功能上的差异,并利用老龄小鼠模型验证其体内骨再生效果。本研究旨在解析亲代细胞衰老对 apoVs 成骨效价的影响,为建立临床级 apoVs 制剂的供体筛选及质控标准提供科学依据。

1 材料和方法

1.1 实验动物

18月龄雌性 C57BL/6 老龄小鼠,购自北京维通利华实验动物技术有限公司,实验动物使用许可证号: SCXK(京)2021-0006,饲养于 SPF 级环境。本研究已获得北京大学生物医学伦理委员会实验动物福利伦理分会的批准(审批号: PUIRB-LA2024088)。

1.2 主要材料与仪器

原代人 BMSCs (7500, Sciencell, 美国), α -MEM 培养基、胎牛血清、胰蛋白酶-EDTA 溶液、青-链霉素双抗 (Gibco, 美国), β -甘油磷酸钠、抗坏血酸、地塞米松、茜素红 (alizarin red S, ARS) 粉末 (Sigma, 美国), TRIzol™ (Invitrogen, 美国), 星形孢菌素 (staurosporine, STS) (Enzo Life Sciences, 美国), 一抗: 兔抗人 CD9、兔抗人 CD63、兔抗人 CD81、兔抗人 Fas (ab236630, ab109201, ab134045, ab133619, Abcam, 美国), 一抗: 兔抗人 p21、鼠抗人 β -actin (10355-1-AP、66009-1-Ig, 三鹰生物, 中国), 二抗: HRP-山羊抗兔、HRP-山羊抗鼠 (ZB-2301, ZB2305, 中杉金桥, 中国), TUNEL 细胞凋亡检测试剂盒 (C003-20, 普利莱, 中国), CCK-8 细胞增殖-毒性检测试剂盒

(CK04, Dojindo, 日本), RNA 逆转录试剂盒 (RR037A, Takara, 日本), 衰老相关 β -半乳糖苷酶 (senescence-associated β -galactosidase, SA- β -gal) 染色试剂盒、BCIP/NBT 碱性磷酸酶 (alkaline phosphatase, ALP) 显色试剂盒 (C0602, P0321S, 碧云天, 中国), ALP 定量测试盒 (A059-3, 建成生物工程研究所, 中国), 激光纳米颗粒跟踪分析仪、分析软件 (Zeta View QUATT, ZetaView® analysis software Version 8.02.31, Particle Metrix, 德国), 透射电镜 (transmission electron microscope, TEM) (HT7700, HITACHI, 日本), 冷冻电镜 (cryo-electron microscopy, cryo-EM) (Titan Krios, FEI, 美国), PCR 梯度基因扩增仪 (EPS5345, Eppendorf, 德国), 实时定量 PCR 仪 (7500, Applied Biosystems, 美国), 微计算机断层扫描 (microcomputer tomography, micro-CT, Inveon, Siemens, 德国)、micro-CT 分析软件 (Inveon Research Workplace, Siemens, 德国)。

1.3 衰老 BMSCs 的体外构建与鉴定

1.3.1 多次传代构建 A-BMSCs BMSCs 培养于含 10% 胎牛血清和 1% 青-链霉素双抗的 α -MEM 培养基,待细胞融合度达 80% 时以 1:3 比例进行细胞传代。根据先前复制性衰老相关研究,将传代至第 4 代及以内的细胞定义为年轻 BMSCs (Y-BMSCs),传代至第 20 代或以上的细胞定义为衰老 BMSCs (A-BMSCs)^[18]。在显微镜下观察 Y-BMSCs 和 A-BMSCs 的形态并采集图像。

1.3.2 Western blot 检测细胞衰老蛋白标志物 p21 为了从分子水平验证细胞周期阻滞情况,提取细胞总蛋白,根据 BCA 蛋白定量试剂盒的说明测定蛋白浓度,通过 Western blot 实验检测细胞周期抑制蛋白 p21 的表达情况。

1.3.3 SA- β -gal 染色和半定量分析 为了鉴定 BMSCs 的细胞衰老状态,将 Y-BMSCs 和 A-BMSCs 以 5×10^4 个/孔的密度接种于 12 孔板内,培养至细胞融合度达 80% 时,按照 SA- β -gal 染色试剂盒的说明进行染色,检测细胞衰老关键标志物 SA- β -gal 的活性。在倒置显微镜下观察并采集高分辨率图像。随后,使用 Image J 软件,通过颜色阈值法对图像进行半定量分析。每组随机选取 5 个视野进行分析。

1.3.4 BMSCs 多向分化 为了评估 BMSCs 衰老后的分化潜能,对 Y-BMSCs 和 A-BMSCs 进行成骨分化诱导和成脂分化诱导培养和后续检测。成骨分化诱导:将 BMSCs 以 2×10^4 个/cm² 的密度接种于 6 孔板

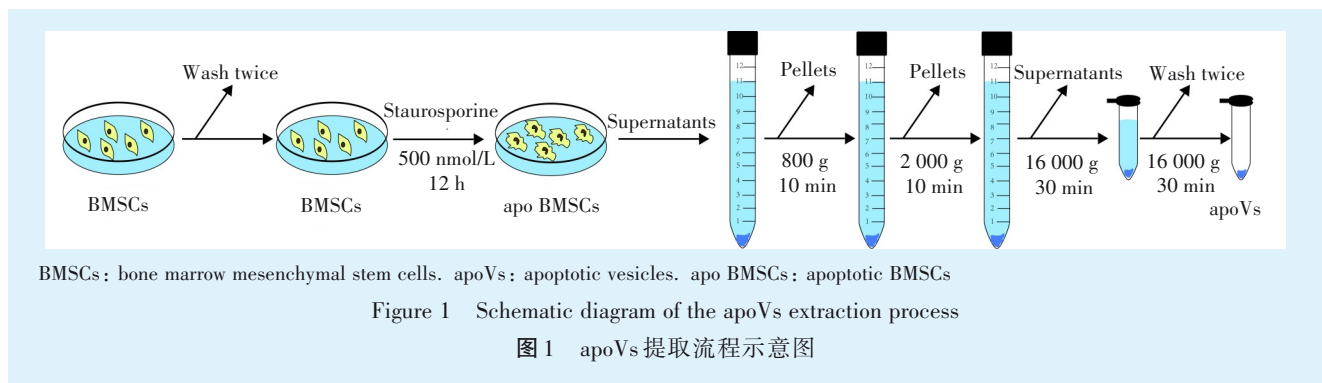
或12孔板。待细胞生长至80%~90%融合时,弃去常规培养基,更换为成骨诱导培养基。根据不同实验目的,持续诱导5~14 d。成脂分化诱导:将BMSCs以 1×10^5 个/孔的密度接种于6孔板中,待细胞生长至100%融合后,继续培养2 d以进行接触抑制。随后更换为成脂诱导培养基。总计培养约14 d后,进行油红O染色和定量检测。

1.4 凋亡诱导和凋亡囊泡的分离提取

1.4.1 TUNEL染色检测BMSCs凋亡 将Y-BMSCs和A-BMSCs培养至90%融合时,更换为含500 nmol/L STS的无血清培养基诱导凋亡12 h(Y-BMSCs组和A-BMSCs组),不加STS为Control组。为验证细胞发生了凋亡,使用TUNEL细胞凋亡检测试剂盒对

处理前后的BMSCs进行染色,用荧光显微镜观察并采集图像。随后,使用Image J软件,对荧光强度进行半定量分析。每个样本组随机选取4个视野进行分析。

1.4.2 apoVs分离提取 为了从凋亡BMSCs培养基中提取纯化的apoVs,通过连续离心和过滤逐步分离^[19]。培养基首先在4℃下800 g离心10 min,随后在4℃下2 000 g离心10 min以去除凋亡细胞碎片。然后收集所得上清液,并在4℃下16 000 g离心30 min以沉淀apoVs,分别为Y-BMSCs来源apoVs(Y-apoVs)和A-BMSCs来源apovs(A-apoVs),随后用0.1 μm过滤的PBS洗涤2次(图1)。



1.5 凋亡囊泡的系统表征

1.5.1 电镜观察 分别使用透射电镜(TEM)和冷冻电镜(cryo-EM)观察apoVs的超微结构和膜形态并采集图像。

1.5.2 纳米颗粒跟踪分析 使用Zeta View测定apoVs的粒径和电位。对于囊泡产量的比较,计数等量(2×10^6 个)Y-BMSCs和A-BMSCs,待细胞贴壁后,诱导细胞凋亡并分离提取apoVs,随后用等量(50 μL)的无菌PBS重悬apoVs,再利用Zeta View测定apoVs微粒数,apoVs微粒数与亲代细胞数的比值即为单个细胞的囊泡产量。

1.5.3 蛋白标志物检测 提取apoVs总蛋白,根据BCA蛋白定量试剂盒的说明测定蛋白浓度,通过Western blot实验检测EVs通用标志物(CD9、CD63、CD81)和凋亡相关标志物Fas的表达情况。

1.6 凋亡囊泡与年轻BMSCs共培养情况的评估

1.6.1 apoVs对Y-BMSCs增殖的影响 将Y-BMSCs以5 000个/孔的密度接种于96孔板,24 h后,根据apoVs的最终添加浓度分为0、50、100、200、400、800 ng/mL组,更换为含上述相应浓度Y-apoVs或

A-apoVs的α-MEM完全培养基(含10%胎牛血清),连续培养7 d,每日使用CCK-8试剂盒在450 nm波长下测量吸光度值,绘制增殖曲线。

1.6.2 Y-BMSCs内吞apoVs 为了评估apoVs能否被靶细胞有效内吞,根据PKH26红色荧光染料试剂盒的说明标记apoVs,将标记后的apoVs与接种在共聚焦皿中的Y-BMSCs共培养,分别设定0、6、12、24 h 4个时间节点,并用鬼笔环肽和DAPI分别标记细胞骨架和细胞核。使用激光扫描共聚焦显微镜观察并采集图像。使用Image J软件,通过颜色阈值法对荧光结果进行半定量分析。每个样本组的每个时点随机选取3个视野进行统计分析。

1.7 凋亡囊泡对年轻BMSCs体外成骨分化的影响

1.7.1 分组与处理 为了评估2组apoVs的体外骨诱导潜力,将Y-BMSCs以 5×10^4 个/孔的密度接种于12孔板,分为4组:增殖培养(proliferation medium, PM)组、成骨诱导(osteogenic induction medium, OM)组、OM + Y-apoVs组和OM + A-apoVs组。参照本课题组前期建立的优化体系^[20],在后两组中加入终浓度为200 ng/mL的apoVs(最适诱导浓

度);7 d时(早期分化阶段)检测 ALP 活性及成骨相关基因的 mRNA 表达水平,14 d时(晚期矿化阶段)检测钙结节,评估成骨效能。

1.7.2 ALP 染色与活性定量 诱导 7 d 后,使用 BCIP/NBT 试剂盒进行 ALP 染色并扫描成像。同时,收集细胞裂解液,按照 ALP 定量测试盒的说明测定 ALP 活性,并以总蛋白浓度进行标准化。

1.7.3 茜素红染色与钙结节定量 诱导 14 d 后,使用 1% ARS 染液(pH 4.2)对钙结节进行染色并扫描成像。随后,使用 1% 氯化十六烷基吡啶溶液溶解

染料,在 562 nm 波长下测定吸光度,并以总蛋白浓度进行标准化。

1.7.4 实时定量 PCR (quantitative real-time PCR, qRT-PCR) 在体外诱导培养 7 d 提取细胞总 RNA,逆转录为 cDNA 后,通过 qRT-PCR 检测成骨相关基因 runt 相关转录因子 2 (runt-related transcription factor 2, RUNX2)、ALP、骨桥蛋白(osteopontin, OPN)、成骨细胞特异性转录因子(osterix, OSX)的 mRNA 表达水平。引物序列见表 1。

表 1 qRT-PCR 引物序列
Table 1 qRT-PCR primer sequences

Gene	Forward primer(5'-3')	Reverse primer(5'-3')
GAPDH	CGGACCAATACGACCAATCCG	AGCCACATCGCTCAGACACC
ALP	GACCTCCTCGGAAGACACTC	TGAAGGGCTTCTTGCTGTG
RUNX2	TCTTAGAACAAATCTGCCCTTT	TGCTTTGGTCTTGAAATCACA
OPN	ACCCTGACCCATCTCAGAAGCA	CTTGAAGGGTCTGTGGGGCTA
OSX	CCTCCTCAGCTCACCTTCTC	GTTGGGAGCCCAATAGAAA

GAPDH: glyceraldehyde-3-phosphate dehydrogenase. ALP: alkaline phosphatase. RUNX2: runt-related transcription factor 2. OPN: osteopontin. OSX: osterix

1.8 动物实验

1.8.1 分组与处理 为了检验 2 组 apoVs 的体内成骨治疗作用,选用 18 月龄的雌性 C57BL/6 老龄小鼠作为老龄性骨质疏松模型^[21]。本课题组在前期研究中确定了 BMSCs 来源 apoVs 治疗骨质疏松的最佳治疗方案^[20],本研究沿用了此方案。18 月龄雌性 C57BL/6 老龄小鼠饲养于 SPF 级环境。使用随机数字表法将小鼠分为 3 组($n = 4$): Control 组、Y-apoVs 组和 A-apoVs 组。

Y-apoVs 组和 A-apoVs 组通过尾静脉每周注射 1 次相应 apoVs (考虑到荧光染料在长周期实验中容易淬灭,且长期多次注射染料可能引入额外的干扰因素,因此使用的是未标记的 apoVs),剂量为 1 mg/kg,连续 8 周,Control 组注射等量(200 μ L)等频次的 PBS。实验结束后处死小鼠,收集股骨样本进行分析。

1.8.2 apoVs 的体内生物分布检测 为了评估 apoVs 在体内的归巢与分布情况,另取 18 月龄 C57BL/6 小鼠并随机分为 3 组($n = 3$): Control 组(注射 PBS)、Y-apoVs 组(注射 PKH26 标记的 Y-apoVs)和 A-apoVs 组(注射 PKH26 标记的 A-apoVs)。

根据 PKH26 红色荧光染料试剂盒的说明,对提取的 Y-apoVs 和 A-apoVs 进行膜标记。将标记后的

apoVs (1 mg/kg) 或等量 PBS (200 μ L) 通过尾静脉注射入各组小鼠体内。在注射 16 h 后,处死小鼠并完整解剖取出主要脏器(心、肝、脾、肺、肾)及双侧股骨。

使用小动物活体成像系统对离体器官进行荧光成像,并分析各器官的荧光辐射效率,以评估 apoVs 在各组织中的蓄积情况。

1.8.3 Micro-CT 分析 使用高分辨率 micro-CT 扫描股骨远端干骺端,选取生长板下方 1.5 mm 处、共 200 个连续切片的区域作为感兴趣区域。通过三维重建和软件定量分析,计算骨体积分数(bone volume fraction, BV/TV)和骨矿物质密度(bone mineral density, BMD)。

1.8.4 组织学染色 将脱钙后的股骨样本进行石蜡包埋并切成 5 μ m 厚的切片。分别进行苏木精-伊红(hematoxylin eosin, H&E)染色和 Masson 三色染色,以评估骨组织形态学和胶原沉积情况。

1.9 统计学分析

所有定量数据均表示为均值 \pm 标准差,每组实验至少重复 3 次。结果用 SPSS 27.0 软件进行单因素方差分析及 Tukey's 事后检验。若方差不齐,则采用 Welch's ANOVA 检验及 Dunnett's T3 法进行事后比较。 $P < 0.05$ 被认为具有统计学意义。

2 结果

2.1 衰老 BMSCs 模型的建立与鉴定

A-BMSCs 细胞模型的建立与鉴定结果见图 2。Y-BMSCs 呈典型纺锤形,排列紧密且呈漩涡状生长;而 A-BMSCs 细胞体积增大,形态扁平不规则,且细胞间连接松散。Western Blot 结果显示,与 Y-BMSCs 相比,A-BMSCs 中 p21 蛋白的表达量显著上调,提示 A-BMSCs 发生了不可逆的细胞周期阻滞,这与复制性衰老的典型特征一致。SA- β -gal 染色和半定量结果证实,A-BMSCs 组中呈蓝色的 SA- β -gal 阳性染色区域面积占比显著高于 Y-BMSCs 组 ($P < 0.000 1$)。Y-BMSCs 在诱导 7 d 后 ALP 染色时表现出显著的蓝紫色染色,而 A-BMSCs 的染色则明显更浅,定量结果与染色结果的趋势一致 ($P < 0.000 1$);经过 14 d 诱导,Y-BMSCs 形成了大面积致密的钙化结节,而 A-BMSCs 形成的钙结节数量显著减少,染色变浅,半定量结果与染色结果的趋势一致 ($P < 0.001$)。在成脂分化方面,经过 14 d 诱导后,在 A-BMSCs 细胞内观察到更多、更大的脂滴,半定量结果与染色结果的趋势一致 ($P < 0.000 1$)。上述结果证实,本研究成功地建立了 BMSCs 复制性衰老模型,A-BMSCs 表现出典型的成骨分化能力减弱、成脂分化能力增强等变化。

2.2 星形孢菌素诱导年轻 BMSCs 和衰老 BMSCs 细胞凋亡

与 Control 组相比,经星形孢菌素(STS)处理后的 Y-BMSCs 组和 A-BMSCs 组均出现大量 TUNEL 阳性细胞。半定量分析的结果进一步表明,Y-BMSCs 与 A-BMSCs 的细胞凋亡率差异无统计学意义(图 3)。以上结果证实星形孢菌素能均一高效地诱导 Y-BMSCs 及 A-BMSCs 发生凋亡。

2.3 年轻 BMSCs 来源凋亡囊泡和衰老 BMSCs 来源凋亡囊泡的系统表征及比较

TEM 和 cryo-EM 结果显示,Y-apoVs 和 A-apoVs 均呈现出典型的双凹圆盘形或球形囊泡结构,具有清晰的双层膜。Western blot 检测证实,两组均高表达 EVs 通用标志物 CD9、CD63 和 CD81,以及凋亡特异性标志物 Fas。ZetaView 测定结果显示,两组 apoVs 的粒径分布集中在 100~500 nm,表面均带负电荷且电位值相近,等量 Y-BMSCs 与 A-BMSCs 产生的 apoVs 微粒数差异无统计学意义 ($P > 0.05$)。稳定性评估结果显示,与新鲜样本相比,在 -80°C 冻存 1 个月样本的蛋白浓度及微粒浓度差异均无统计学意义 ($P > 0.05$)(图 4)。以上结

果表明,本研究成功地从 Y-BMSCs 和 A-BMSCs 中分离出了纯度较高的 apoVs,2 种 apoVs 在 -80°C 下均可稳定储存至少 1 个月,且亲代细胞衰老未显著改变其衍生 apoVs 的物理表征及分泌产量。

2.4 年轻 BMSCs 来源凋亡囊泡和衰老 BMSCs 来源凋亡囊泡的生物安全性比较

与不添加 apoVs 相比,在 200 ng/mL 及以下的浓度范围内,2 种 apoVs 对 Y-BMSCs 的增殖均无显著影响;当浓度升高至 400 ng/mL 时,A-apoVs 开始抑制细胞增殖 ($P < 0.05$);在 800 ng/mL 时,2 种 apoVs 均显著抑制细胞增殖 ($P < 0.01$)(图 5)。综上,尽管在低浓度下 2 种 apoVs 均表现出良好的生物相容性,但源自衰老 BMSCs 的 A-apoVs 在较高浓度下更早显示出细胞毒性,提示 A-apoVs 的生物安全性相对较低。考虑到促分化实验的控制变量需求及细胞安全性,选用 200 ng/mL 作为后续体外实验的安全有效浓度。

2.5 年轻 BMSCs 对凋亡囊泡的内吞情况

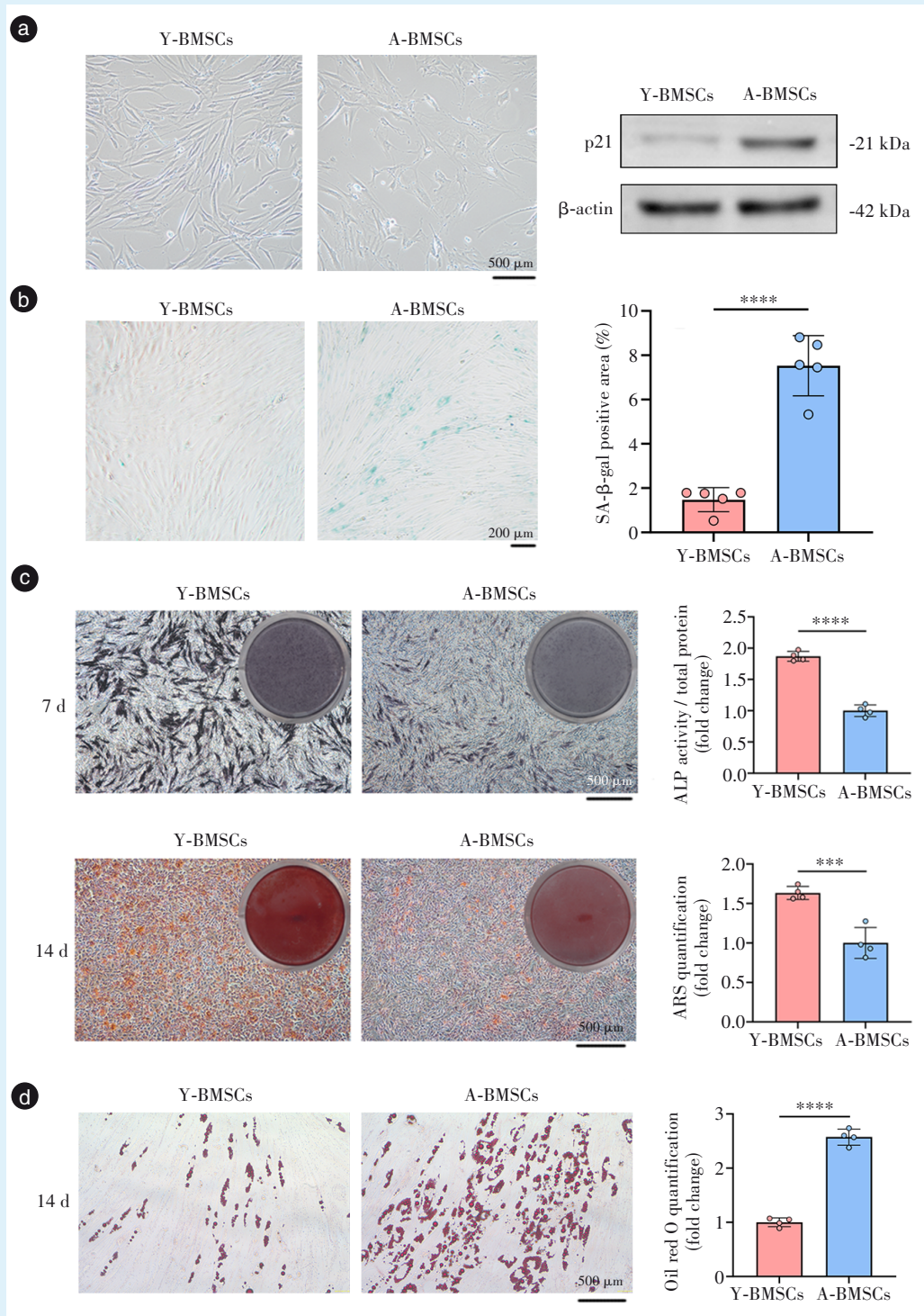
在共培养 6 h 后,即可在靶细胞 Y-BMSCs 的胞浆区域观察到红色荧光信号,且随着时间的推移直至 24 h,胞内的红色荧光点逐渐增多、增强。半定量分析结果证实,随着时间推移至 24 h,Y-BMSCs 对 2 种囊泡的摄取均不断增加,并且在共培养 24 h 内,Y-BMSCs 对 2 种囊泡的内吞差异无统计学意义 ($P > 0.05$)(图 6)。以上结果表明,Y-BMSCs 能有效地内吞 2 种 apoVs。

2.6 年轻 BMSCs 来源凋亡囊泡具有比衰老 BMSCs 来源凋亡囊泡更强的体外骨诱导潜力

Y-BMSCs 成骨分化结果如图 7 所示。ALP 染色结果显示,OM + Y-apoVs 组和 OM + A-apoVs 组的 ALP 染色强度均高于 OM 组,且 OM + Y-apoVs 组的染色更深。ALP 活性定量分析结果与染色观察一致,各组活性强度依次为:OM + Y-apoVs 组 > OM + A-apoVs 组 > OM 组 > PM 组 ($P < 0.01$)。

ARS 染色结果显示,与 OM 组相比,OM + A-apoVs 组和 OM + Y-apoVs 组均形成了更大、更密集红色钙盐沉积区域。其中,OM + Y-apoVs 组的矿化程度更为显著。定量分析证实了钙化水平的趋势同样为:OM + Y-apoVs 组 > OM + A-apoVs 组 > OM 组 > PM 组 ($P < 0.01$)。

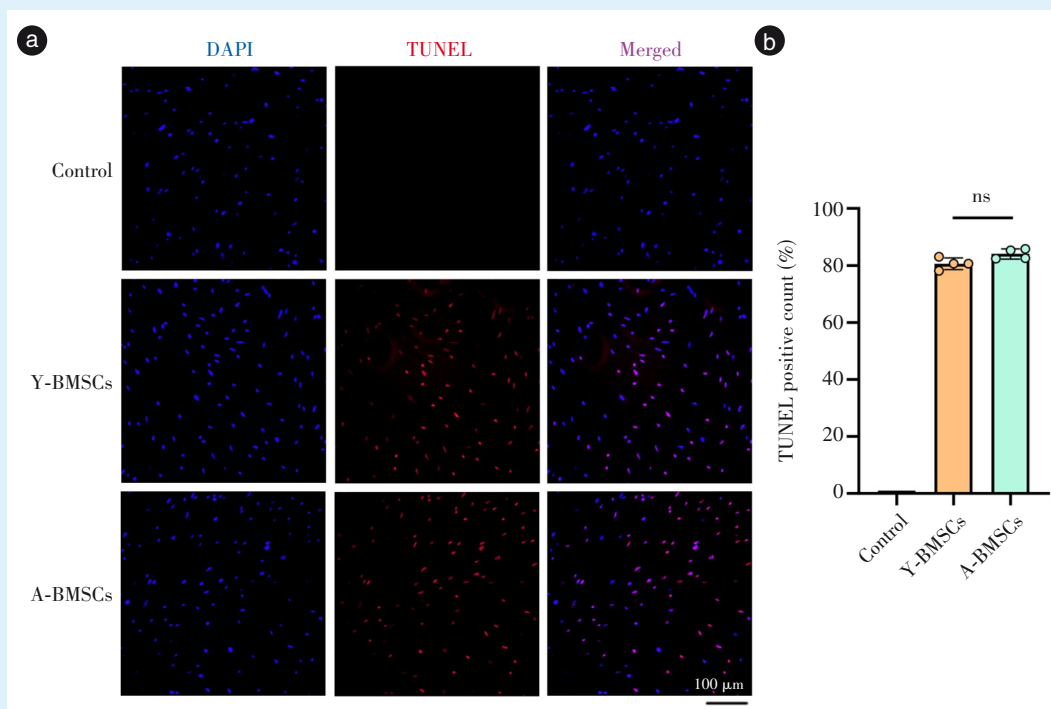
qRT-PCR 对关键成骨相关转录因子 mRNA 表达的检测结果显示,与 PM 组相比,OM 组、OM + A-apoVs 组和 OM + Y-apoVs 组成骨标志基因 (RUNX2、ALP、OPN 和 OSX) 的表达均显著上调。



a: representative microscopic images of cell morphology for Y-BMSCs and A-BMSCs (scale bar = 500 μm) and expression levels of the senescence marker protein p21 determined by Western blot. Y-BMSCs exhibited a typical spindle-shaped morphology, were closely arranged, and grew in a vortex-like manner. A-BMSCs exhibited a flattened and irregular morphology. b: microscopic images of SA-β-gal staining (scale bar = 200 μm) and semi-quantitative results (n = 5). Blue precipitates indicated senescent cells. c: ALP staining and quantification (scale bar = 500 μm, n = 4), and ARS staining and semi-quantification (scale bar = 500 μm, n = 4). Blue-purple staining indicated ALP activity; red mineralized nodules indicated calcium deposition. d: oil red O staining and semi-quantification (scale bar = 500 μm, n = 4). Red lipid droplets indicated adipogenic differentiation. *** $P < 0.001$, **** $P < 0.0001$ vs. the Y-BMSCs group. Y-BMSCs: young BMSCs group. A-BMSCs: aging BMSCs group. SA-β-gal: senescence-associated β-galactosidase. ALP: alkaline phosphatase. ARS: alizarin red S. BMSCs: bone marrow mesenchymal stem cells

Figure 2 Establishment and identification of the A-BMSC model

图2 A-BMSCs 细胞模型的建立与鉴定



a: fluorescence images of TUNEL staining after apoptosis induction. Nuclei were labeled with DAPI (blue), and apoptotic cells were labeled red (scale bar = 100 μm). Red fluorescence indicated DNA fragmentation in apoptotic cells. b: semi-quantitative analysis of TUNEL staining (n = 4). ns: no significant difference (P > 0.05). Control: BMSCs group without STS treatment. Y-BMSCs: young BMSCs group treated with STS. A-BMSCs: aging BMSCs group treated with STS. STS: staurosporine. TUNEL: terminal deoxynucleotidyl transferase dUTP nick end labeling. BMSCs: bone marrow mesenchymal stem cells

Figure 3 TUNEL staining validation of STS-induced apoptosis in BMSCs

图3 星形孢菌素诱导BMSCs凋亡后TUNEL染色

OM + Y-apoVs组中所有检测基因的表达水平均为最高,显著优于OM组,而OM + A-apoVs组的促进成骨基因表达效果则介于OM + Y-apoVs组和OM组之间(P < 0.05)。

上述结果表明,BMSCs来源的apoVs具有直接的体外骨诱导作用,且该作用与来源细胞的衰老状态密切相关,Y-apoVs展现出更强的成骨诱导能力。

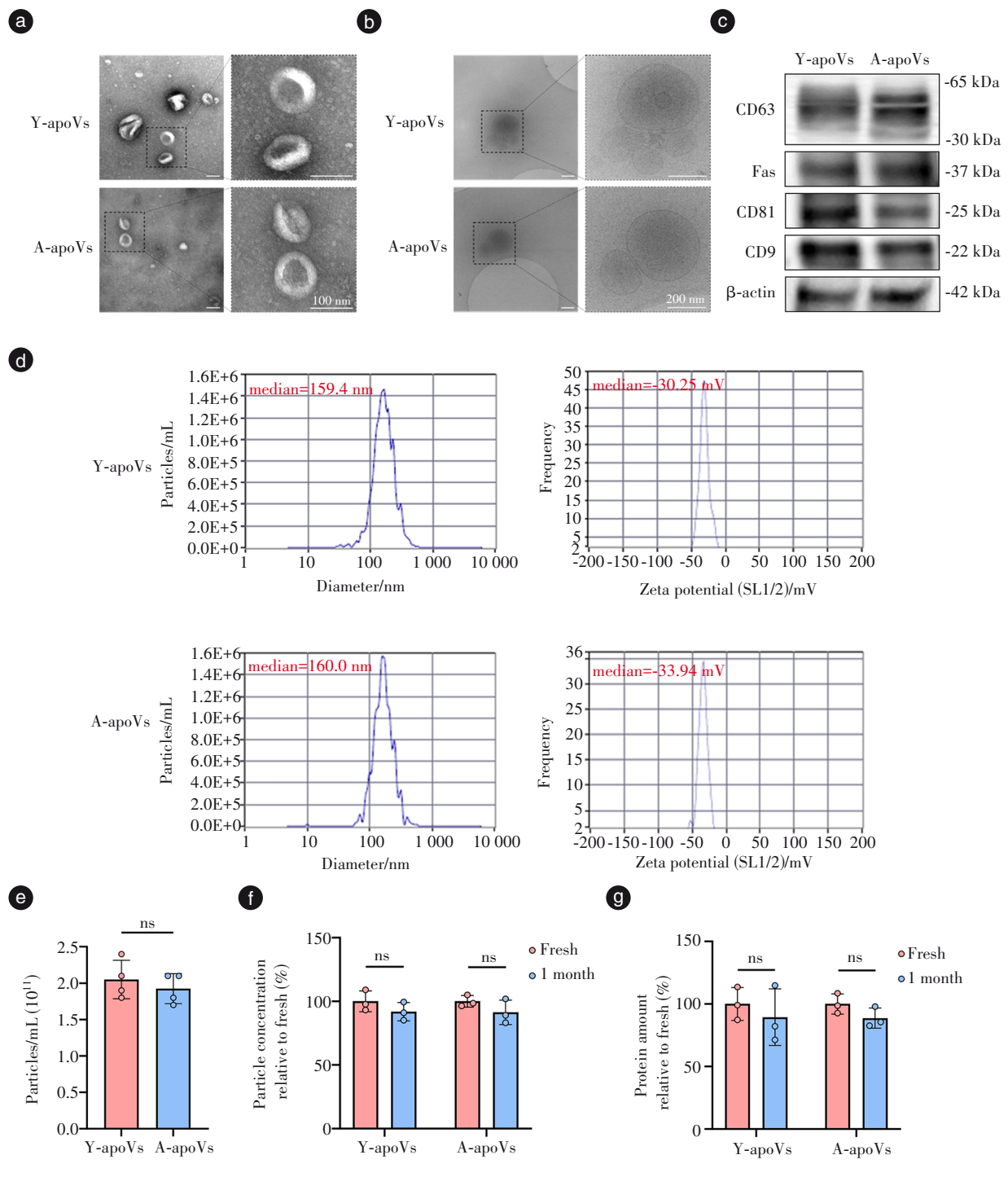
2.7 年轻BMSCs来源凋亡囊泡治疗老龄性骨质疏松的效果优于衰老BMSCs来源凋亡囊泡

离体荧光成像结果显示,尾静脉注射16 h后,PKH26标记的apoVs(红色荧光)在各主要脏器中呈现差异化分布。半定量分析结果显示,肝脏表现出最高的荧光强度。这一现象符合细胞外囊泡的药代动力学特征,即肝脏作为机体主要的网状内皮系统器官,是外源性囊泡代谢和清除的主要场所^[7]。尽管存在肝脏的代谢清除作用,在股骨组织中仍检测到了显著的荧光信号积聚(图8a),且Y-apoVs与A-apoVs在骨组织的归巢效率差异无统

计学意义。这证实了系统给药的apoVs,无论是Y-BMSCs还是A-BMSCs来源,均能够有效突破代谢屏障并到达骨组织发挥治疗作用。

通过micro-CT对各组小鼠股骨远端的骨微结构进行了三维重建和分析。从代表性的三维图像中可以看到(图8b),与Control组相比,A-apoVs组的骨小梁网络虽有一定程度的改善,但Y-apoVs组表现出更显著的骨量增加,其骨小梁结构更致密、连接更完整。骨密度分析的定量结果进一步证实了上述观察(图8c),Y-apoVs组的BMD和BV/TV均显著高于Control组和A-apoVs组(P < 0.000 1);A-apoVs组的各项指标虽优于Control组,但其改善效果有限,与Y-apoVs组存在显著差距(P < 0.001)。

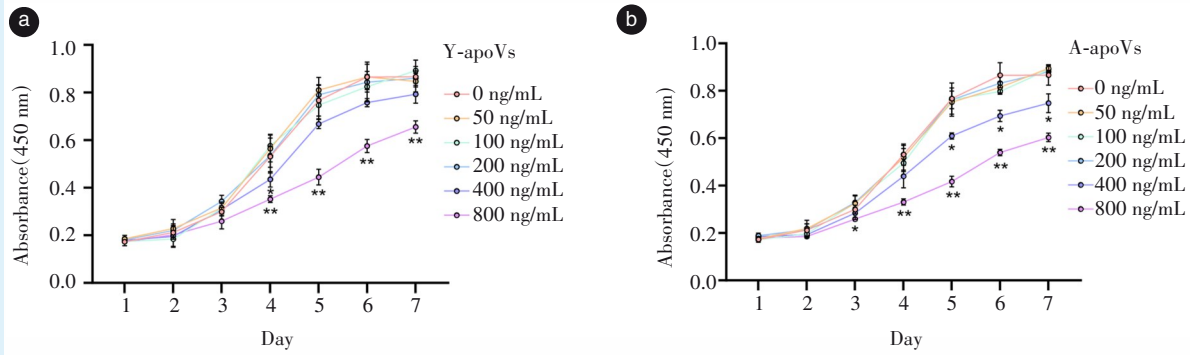
对脱钙后的股骨切片进行了H&E和Masson三色染色。H&E染色结果(图8d)显示,Control组的骨小梁稀疏、变细,骨髓腔内脂肪细胞数量较多,呈现出典型的骨质疏松样改变,A-apoVs组的骨小梁形态略有改善,Y-apoVs组的骨小梁不仅数量增多、厚度增加,而且排列更为规整有序,骨髓腔内



a: TEM images (scale bar = 100 nm). ApoVs displayed a typical cup-shaped morphology. b: cryo-EM images (scale bar = 200 nm). Both Y-apoVs and A-apoVs exhibited a typical biconcave discoid morphology and bilayer membrane structures. c: both groups highly expressed universal EV markers (CD9, CD63, CD81) and the apoptotic marker Fas. d: the particle size distribution of both apoVs ranged from 100 to 500 nm, and both carried negative surface charges with similar potentials. e: quantitative analysis of the apoV yield showing no significant difference in the particle number of apoVs derived from equal amounts of young and aging BMSCs ($n = 4$). f&g: comparison of the protein concentration (f) and particle concentration (g) showing no significant difference between freshly isolated apoVs (Fresh) and apoVs stored at -80°C for 1 month ($n = 3$). ns: no significant difference ($P > 0.05$) vs. the Y-apoV group. Y-apoVs: apoVs derived from young BMSCs. A-apoVs: apoVs derived from aging BMSCs. TEM: transmission electron microscope. cryo-EM: cryo-electron microscopy. BMSCs: bone marrow mesenchymal stem cells

Figure 4 Phenotypic characterization of Y-apoVs and A-apoVs

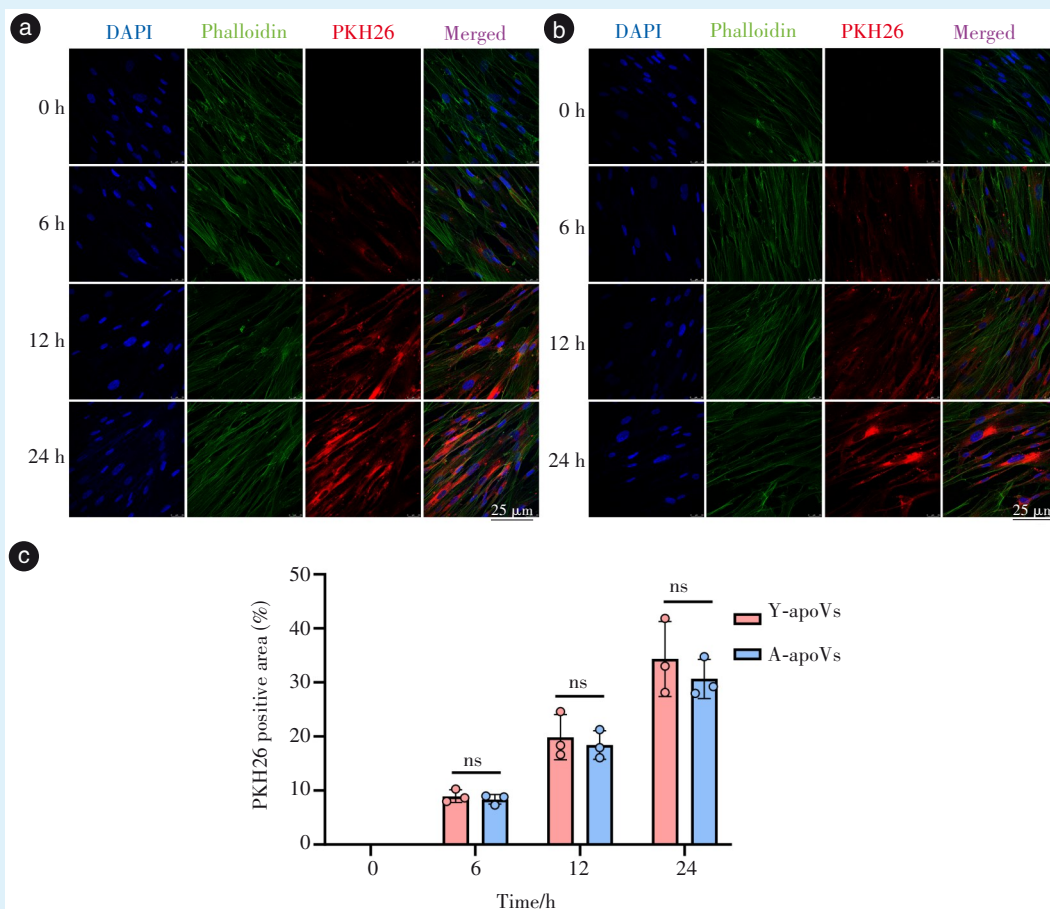
图4 Y-apoVs 和 A-apoVs 的系统表征



a&b: compared with 0 ng/mL group, both Y-apoVs and A-apoVs had no significant effect on the proliferation of Y-BMSCs at concentrations of 200 ng/mL and below; when the concentration increased to 400 ng/mL, A-apoVs began to inhibit cell proliferation; at 800 ng/mL, both apoVs significantly inhibited cell proliferation. * $P < 0.05$, ** $P < 0.01$ vs. the 0 ng/mL group. Y-BMSCs were cultured in mediums containing final apoVs concentrations of 0, 50, 100, 200, 400, and 800 ng/mL. BMSCs: bone marrow mesenchymal stem cells. Y-apoVs: apoVs derived from young BMSCs (Y-BMSCs); A-apoVs: apoVs derived from aging BMSCs. apoVs: apoptotic vesicles

Figure 5 Effect of apoVs with different concentrations on the proliferation of Y-BMSCs

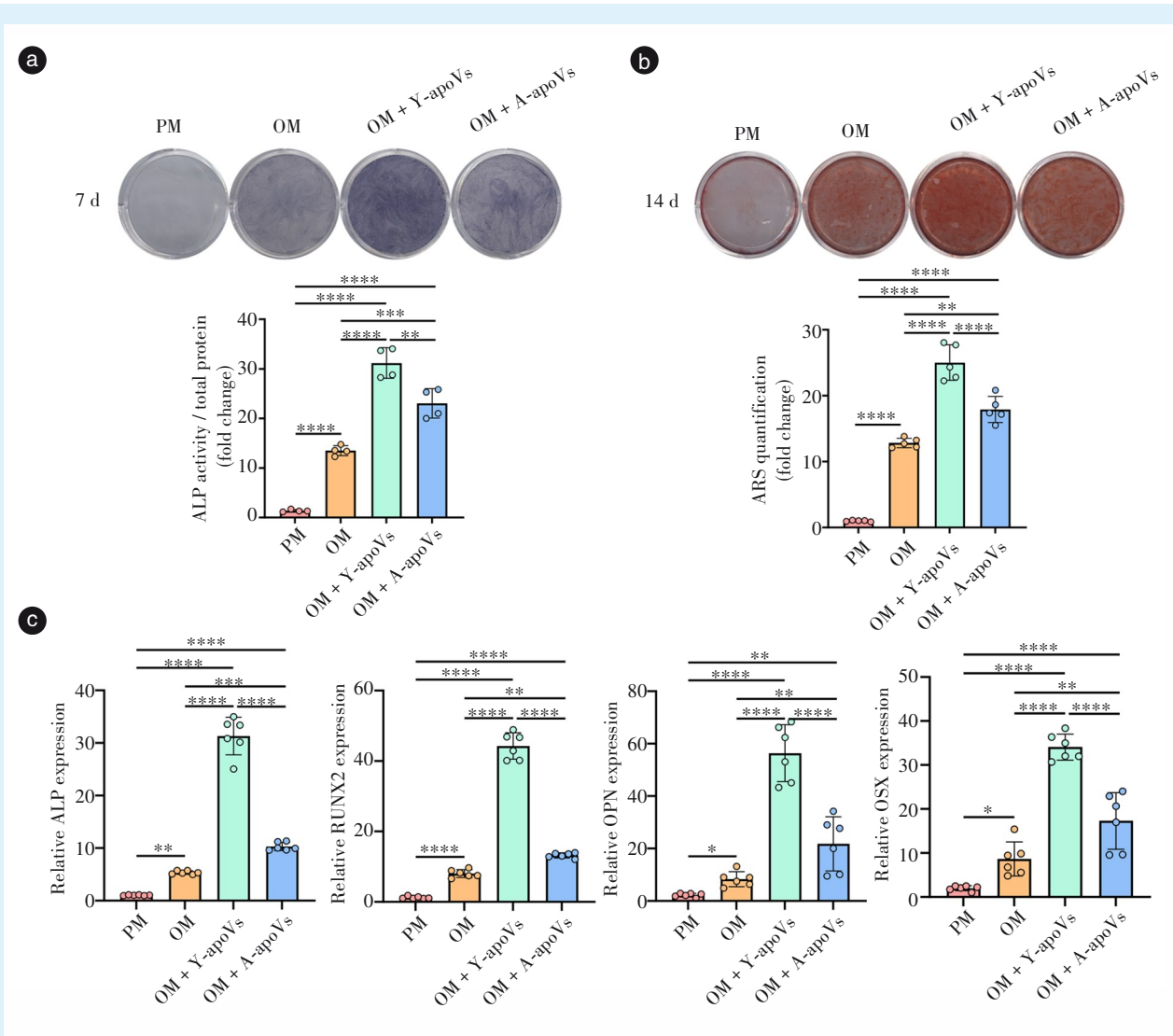
图5 不同浓度 apoVs 处理对 Y-BMSCs 增殖的影响



a&b: uptake of Y-apoVs (a) and A-apoVs (b) by Y-BMSCs after co-culture for 6, 12, and 24 hours. Nuclei were labeled with DAPI (blue), the cytoskeleton with Phalloidin (green), and apoVs with PKH26 (red) (scale bar = 25 μ m). Red fluorescence in the cytoplasm indicated the uptake of apoVs by Y-BMSCs. c: semi-quantitative analysis of apoVs uptake by Y-BMSCs ($n = 3$). ns: no significant difference ($P > 0.05$). Y-apoVs: Y-BMSCs co-cultured with Y-apoVs. A-apoVs: Y-BMSCs co-cultured with A-apoVs. BMSCs: bone marrow mesenchymal stem cells

Figure 6 Uptake of Y-apoVs and A-apoVs by Y-BMSCs

图6 Y-BMSCs 对 Y-apoVs 和 A-apoVs 的内吞情况



a: ALP staining and quantitative analysis ($n = 4$). b: ARS staining and semi-quantitative analysis ($n = 5$). c: mRNA expression levels of osteogenesis-related genes (RUNX2, ALP, OPN, and OSX) ($n = 6$). * $P < 0.05$, ** $P < 0.01$, *** $P < 0.001$, **** $P < 0.0001$. PM: proliferation medium; OM: osteogenic induction medium; OM + Y-apoVs: Y-BMSCs cultured in OM with Y-apoVs. OM + A-apoVs: Y-BMSCs cultured in OM with A-apoVs. Y-apoVs: apoVs derived from young BMSCs (Y-BMSCs); A-apoVs: apoVs derived from aging BMSCs. apoVs: apoptotic vesicles. BMSCs: bone marrow mesenchymal stem cells. ALP: alkaline phosphatase. RUNX2: runt-related transcription factor 2. OPN: osteopontin. OSX: osterix

Figure 7 Y-apoVs more effectively promote osteogenic differentiation of Y-BMSCs *in vitro*

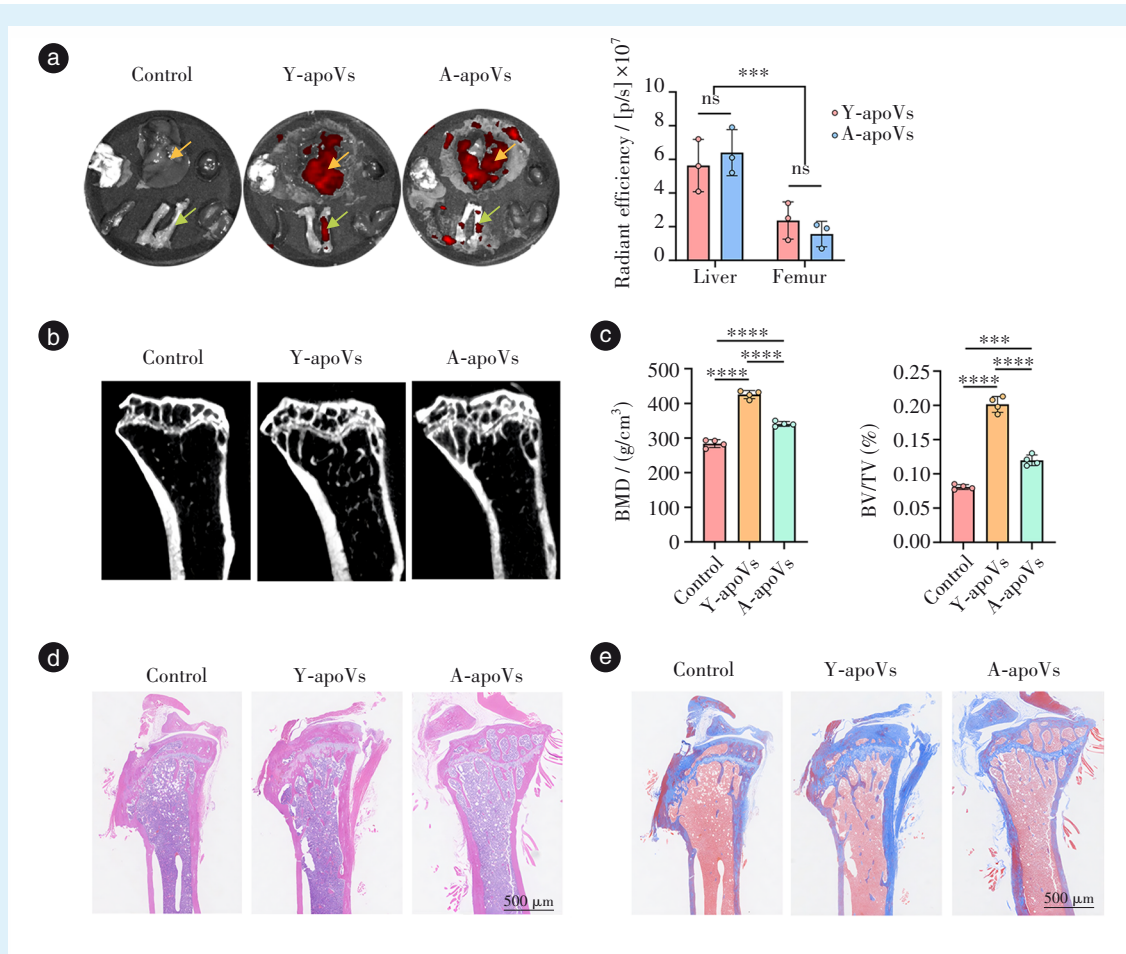
图7 Y-apoVs在体外更有效地促进Y-BMSCs成骨分化

的造血组织也更为丰富。Masson三色染色进一步评估了骨基质中胶原蛋白的沉积情况(图8e), Y-apoVs组的骨小梁区域呈现出较深的蓝色染色,表明其胶原纤维沉积和骨基质矿化水平更高, A-apoVs组的蓝色染色强度介于Control组和Y-apoVs组之间。

体内实验结果证实,尾静脉输注的Y-apoVs能够显著促进老龄小鼠的骨再生,从而逆转年龄相关的骨量丢失。

3 讨论

本研究揭示了BMSCs衍生的apoVs在骨再生中的治疗效能显著受到亲代细胞生物学年龄的调控。BMSCs来源的apoVs在调节骨免疫微环境及促进骨再生方面展现出独特优势^[22]。相较于外泌体, apoVs具有更高的制备效率和独特的分子内容物,更适于口腔临床对骨修复材料的大规模需求,是极具前景的口腔骨再生生物制剂。既往研究表明BMSCs衰老会导致其本身的成骨分化能力减弱^[23]及旁分泌功能改变^[24]。本研究证实细胞衰老



a: biodistribution of apoVs after tail vein injection and semi-quantitative analysis of the average radiant efficiency of PKH26-labeled apoVs in different tissues ($n = 3$). The strongest red fluorescence signal was observed in liver tissue (yellow arrows); distinct red fluorescence was also visible in the femur (green arrows). b: representative 3D reconstruction micro-CT images of the distal femoral metaphysis for each group ($n = 4$). The control group showed sparse trabeculae; the Y-apoV group displayed the densest and most interconnected trabecular microstructure (gray-white areas). c: micro-CT bone density analysis ($n = 4$). d: H&E staining images of femoral sections for each group ($n = 4$, scale bar = 500 μm). Compared with the abundant adipocytes and fractured trabeculae in the control group, the trabeculae (pink) in the Y-apoV group were significantly thickened, increased, and regularly arranged, while the improvement in the A-apoV group was less evident. e: Masson's staining images of femoral sections for each group ($n = 4$, scale bar = 500 μm). Abundant deep blue collagen deposition was observed in the new bone matrix of the Y-apoV group, with staining extent and intensity higher than those in the A-apoV and control groups. ns: no significant difference ($P > 0.05$), *** $P < 0.001$, **** $P < 0.0001$ for comparisons between groups. Control group: aged mice injected with phosphate-buffered saline. Y-apoVs group: aged mice injected with Y-apoVs. A-apoVs group: aged mice injected with A-apoVs. Y-apoVs: apoVs derived from young BMSCs; A-apoVs: apoVs derived from aging BMSCs. apoVs: apoptotic vesicles

Figure 8 Y-apoVs effectively improve the bone tissue regeneration of aged mice *in vivo*

图8 Y-apoVs在体内有效促进老龄小鼠的骨再生

并不会显著影响 apoVs 的物理表征,但会显著削弱 apoVs 的骨诱导功能,表明细胞衰老的负面效应可通过其分泌的 apoVs 进行传递。本研究的独特贡献在于,将“亲代细胞衰老”这一变量引入 apoVs 的质量控制研究中。本研究发现提示在开发基于 apoVs 的无细胞疗法时,供体细胞的衰老程度是决定剂骨再生效价的核心变量,为 apoVs 制剂的标准化制备提供了关键的数据支持。

3.1 衰老 BMSCs 模型的构建与验证

研究表明,无论是机体生理性衰老还是体外长期传代, BMSCs 均会发生衰老^[25-26]。本研究通过体外连续传代构建了复制性衰老模型,主要模拟了端粒缩短和累积损伤导致的细胞周期停滞。一方面,采用多维度的评估标准验证了体外模型的衰老表型:形态学改变、SA- β -gal 染色阳性、衰老关键蛋白 p21 表达上调,成骨成脂分化能力的失衡,

这些数据支持了本研究中复制性衰老模型的有效性,也与体内生理性衰老的细胞特征高度一致^[27-28]。另一方面,机体生理性衰老反映了生物体随时间的生理衰退,涉及不仅是细胞自身的变化,还包括外在因素,如系统性炎症、微环境重塑以及由终生暴露于内在和外在信号形成的表观遗传漂移^[29]。体外复制性衰老模型能有效隔离这些系统因素,反映细胞内在的衰老因素,初步揭示细胞自主性衰老对其衍生 apoVs 功能的主要影响^[30-31]。在探究 apoVs 体外与细胞共培养相关实验中,为了排除靶细胞自身衰老状态对其响应能力的干扰,本研究统一选用 Y-BMSCs 作为靶细胞,从而严格控制“囊泡亲代细胞的衰老状态”这一核心变量,以明确评估亲代细胞衰老对 apoVs 生物学功能的直接影响。

3.2 亲代细胞衰老削弱凋亡囊泡的生物学功能

探究 apoVs 功能差异的生物学基础是理解其再生机制的关键。一个有趣的发现是, Y-apoVs 和 A-apoVs 在形态、粒径、电位、产量以及经典蛋白标志物(CD9、CD63、CD81、Fas)的表达水平差异均无统计学意义,这说明传统的物理表征不足以区分其功能优劣。基于本课题组前期研究及领域内文献^[32-33],本研究提出“内容物决定功能”的假说: apoVs 的治疗潜能取决于其包裹的特异性分子内容物。既往研究表明, Y-BMSCs 来源的 apoVs 富含促再生的 miRNA(如 miR-328-3p、miR-1324 等多种 miRNA),并通过激活关键成骨信号通路(如 Wnt/ β -catenin 和 SMAD1/5 等)来调控骨代谢^[7, 20]。本课题组推测,随着细胞衰老,这些关键的促再生“内容物”在 A-apoVs 中通过选择性分选机制被丢失;或者,根据衰老相关分泌表型理论^[34], A-apoVs 可能富集了某些对成骨有抑制作用的炎症因子或衰老传递信号,从而对其受体细胞产生了“旁观者效应”,抑制了骨再生^[35]。本研究通过功能实验已验证了这种生物活性的丧失,后续研究应重点关注 apoVs 内容物随细胞衰老的动态演变。

3.3 凋亡囊泡质量控制的临床转化意义

本研究结果对于推动 apoVs 在口腔骨修复中的临床转化具有一定的指导意义。生物制剂的“供体异质性”是制约其标准化的瓶颈^[36-37]。本研究数据显示,物理表征(如形态、粒径、电位及经典 EVs 标志物 CD9、CD63、CD81)无法区分 Y-apoVs 与 A-apoVs 的功能差异,如体外诱导 BMSCs 表达成骨基因及形成钙结节的能力、体内促进老龄小鼠骨

小梁重建的治疗效能,因此,仅凭物理参数不足以作为放行标准。为了确保临床级 apoVs 制剂的骨再生效价,本课题组建议建立“供体溯源-制备工艺-功能标志物”的三级质控体系:①供体筛选:严格限定供体生理年龄,优先选择年轻供体(如拔除智齿的青少年患者)来源的干细胞;②工艺控制:设定严格的体外扩增代次限制(建议控制在 P5 代以内),以避免体外长期扩增导致的复制性衰老;③分子放行:在制备前对亲代细胞进行年轻状态核查。基于本研究结果,建议将细胞周期阻滞蛋白(p21)低表达、SA- β -gal 染色阴性以及保留正常的成骨/成脂分化平衡作为核心检测指标。除了检测基础的衰老标志物外,在未来,筛选出影响 apoVs 功能的关键“效价指示分子”后^[38-39],还能定向剔除功能性衰老的细胞批次,确保终产品的治疗效价。只有通过上述多维度评估的年轻态细胞,方可用于制备具有高效骨再生能力的 apoVs 制剂。

本研究仍存在一定的局限性。首先,尚未通过组学技术鉴定出导致 Y-apoVs 和 A-apoVs 功能差异的具体分子靶点(如特定的差异蛋白或 miRNA),筛选并验证这些关键的“效价指示分子”,这将是本课题组下一步的工作重点。其次,未来的研究需在大型动物模型或人源样本中进一步验证结论的普适性。

综上所述,亲代细胞的衰老状态是决定 apoVs 骨诱导特性的关键要素。本研究强调了在开发口腔骨再生 apoVs 生物制剂时,必须重视供体细胞的生命周期状态管理。通过严格筛选年轻供体或控制细胞代次,可显著提升 apoVs 的骨再生治疗效能。

【Author contributions】 Zhu L performed the experiments and wrote the manuscript. Jiang YH and Zhang X designed the study, evaluated the data, and reviewed the manuscript. All authors read and approved the final manuscript as submitted.

参考文献

- [1] Aquino-Martinez R. The emerging role of accelerated cellular senescence in periodontitis[J]. J Dent Res, 2023, 102(8): 854-862. doi: 10.1177/00220345231154567.
- [2] Pius AK, Toya M, Gao Q, et al. Effects of aging on osteosynthesis at bone - implant interfaces[J]. Biomolecules, 2023, 14(1): 52. doi: 10.3390/biom14010052.
- [3] Ma Y, Wang S, Wang H, et al. Mesenchymal stem cells and dental implant osseointegration during aging: from mechanisms to therapy [J]. Stem Cell Res Ther, 2023, 14(1): 382. doi: 10.1186/s13287-

- 023-03611-1.
- [4] 段星祥, 张瑞, 贺燕, 等. 间充质干细胞的细胞治疗策略研究进展[J]. 口腔疾病防治, 2023, 31(10): 745-750. doi: [10.12016/j.issn.2096-1456.2023.10.009](https://doi.org/10.12016/j.issn.2096-1456.2023.10.009).
Duan XX, Zhang R, He Y, et al. Progress on the cell therapy strategy of mesenchymal stem cells[J]. J Prev Treat Stomatol Dis, 2023, 31(10): 745-750. doi: [10.12016/j.issn.2096-1456.2023.10.009](https://doi.org/10.12016/j.issn.2096-1456.2023.10.009).
- [5] Fu Y, He Y, Wu D, et al. Apoptotic vesicles: emerging concepts and research progress in physiology and therapy[J]. Life Med, 2023, 2(2): lnad013. doi: [10.1093/lifemedi/lnad013](https://doi.org/10.1093/lifemedi/lnad013).
- [6] Zheng C, Sui B, Zhang X, et al. Apoptotic vesicles restore liver macrophage homeostasis to counteract type 2 diabetes[J]. J Extracell Vesicles, 2021, 10(7): e12109. doi: [10.1002/jev2.12109](https://doi.org/10.1002/jev2.12109).
- [7] Liu D, Kou X, Chen C, et al. Circulating apoptotic bodies maintain mesenchymal stem cell homeostasis and ameliorate osteopenia via transferring multiple cellular factors[J]. Cell Res, 2018, 28(9): 918-933. doi: [10.1038/s41422-018-0070-2](https://doi.org/10.1038/s41422-018-0070-2).
- [8] Wang M, Gui H, Hu Z, et al. Apoptotic vesicles act as natural anti-bacterial agents for infected wound healing by interfering with the bacterial catabolic process[J]. Nano Res, 2025, 18(10): 1-15. doi: [10.26599/nr.2025.94907776](https://doi.org/10.26599/nr.2025.94907776).
- [9] Ye Q, Qiu X, Wang J, et al. MSCs-derived apoptotic extracellular vesicles promote muscle regeneration by inducing pannexin 1 channel-dependent creatine release by myoblasts[J]. Int J Oral Sci, 2023, 15(1): 7. doi: [10.1038/s41368-022-00205-0](https://doi.org/10.1038/s41368-022-00205-0).
- [10] Luo W, Li H, Zhang P, et al. Apoptotic bodies derived from human umbilical cord mesenchymal stem cells improve recovery from myocardial infarction in swine[J]. Autophagy, 2026, 22(3): 603-622. doi: [10.1080/15548627.2025.2536449](https://doi.org/10.1080/15548627.2025.2536449).
- [11] Jiang Y, Zhu Y, Shao Y, et al. Platelet-derived apoptotic vesicles promote bone regeneration via Golgi phosphoprotein 2 (GOLPH2)-AKT signaling axis[J]. ACS Nano, 2023, 17(24): 25070-25090. doi: [10.1021/acsnano.3c07717](https://doi.org/10.1021/acsnano.3c07717).
- [12] Jiang T, Xia Y, Wang W, et al. Apoptotic bodies inhibit inflammation by PDL1-PD1-mediated macrophage metabolic reprogramming[J]. Cell Prolif, 2024, 57(1): e13531. doi: [10.1111/cpr.13531](https://doi.org/10.1111/cpr.13531).
- [13] Tian G, Yin H, Zheng J, et al. Promotion of osteochondral repair through immune microenvironment regulation and activation of endogenous chondrogenesis via the release of apoptotic vesicles from donor MSCs[J]. Bioact Mater, 2024, 41: 455-470. doi: [10.1016/j.bioactmat.2024.07.034](https://doi.org/10.1016/j.bioactmat.2024.07.034).
- [14] Jiang Y, Li X, Huang R, et al. Lyophilized apoptotic vesicles improve hemostasis and bone regeneration in traumatic patients with impacted third molar extraction[J]. Mol Ther, 2025, 33(6): 2931-2944. doi: [10.1016/j.ymthe.2025.02.033](https://doi.org/10.1016/j.ymthe.2025.02.033).
- [15] Welsh JA, Goberdhan DCI, O'Driscoll L, et al. Minimal information for studies of extracellular vesicles (MISEV2023): from basic to advanced approaches[J]. J Extracell Vesicles, 2024, 13(2): e12404. doi: [10.1002/jev2.12404](https://doi.org/10.1002/jev2.12404).
- [16] 王惠, 朱悦, 张帅帅, 等. 负压调控骨髓间充质干细胞 apoVs 差异 microRNA 表达谱[J]. 医用生物力学, 2025, 40(4): 886-894. doi: [10.16156/j.1004-7220.2025.04.013](https://doi.org/10.16156/j.1004-7220.2025.04.013).
Wang H, Zhu Y, Zhang SS, et al. Negative pressure-regulated mi-croRNA expression in apoptotic vesicles derived from bone marrow mesenchymal stem cells[J]. J Med Biomech, 2025, 40(4): 886-894. doi: [10.16156/j.1004-7220.2025.04.013](https://doi.org/10.16156/j.1004-7220.2025.04.013).
- [17] Zhang J, Cai Z, Feng F, et al. Age-different BMSCs-derived exosomes accelerate tendon-bone interface healing in rotator cuff tears model[J]. Gene, 2024, 895: 148002. doi: [10.1016/j.gene.2023.148002](https://doi.org/10.1016/j.gene.2023.148002).
- [18] Izadpanah R, Kaushal D, Kriedt C, et al. Long-term in vitro expansion alters the biology of adult mesenchymal stem cells[J]. Cancer Res, 2008, 68(11): 4229-4238. doi: [10.1158/0008-5472.CAN-07-5272](https://doi.org/10.1158/0008-5472.CAN-07-5272).
- [19] Chen D, Zhao Z, Zhang K, et al. Protocol for differential centrifugation-based separation and characterization of apoptotic vesicles derived from human mesenchymal stem cells[J]. STAR Protoc, 2022, 3(4): 101695. doi: [10.1016/j.xpro.2022.101695](https://doi.org/10.1016/j.xpro.2022.101695).
- [20] Zhu Y, Yang K, Cheng Y, et al. Apoptotic vesicles regulate bone metabolism via the miR1324/SNX14/SMAD1/5 signaling axis[J]. Small, 2023, 19(16): e2205813. doi: [10.1002/smll.202205813](https://doi.org/10.1002/smll.202205813).
- [21] Piemontese M, Almeida M, Robling AG, et al. Old age causes de novo intracortical bone remodeling and porosity in mice[J]. JCI Insight, 2017, 2(17): e93771. doi: [10.1172/jci.insight.93771](https://doi.org/10.1172/jci.insight.93771).
- [22] Li X, Jiang Y, Liu X, et al. Mesenchymal stem cell-derived apoptotic bodies alleviate alveolar bone destruction by regulating osteoclast differentiation and function[J]. Int J Oral Sci, 2023, 15(1): 51. doi: [10.1038/s41368-023-00255-y](https://doi.org/10.1038/s41368-023-00255-y).
- [23] Zheng L, He S, Wang H, et al. Targeting cellular senescence in aging and age-related diseases: challenges, considerations, and the emerging role of senolytic and senomorphic therapies[J]. Aging Dis, 2024, 15(6): 2554-2594. doi: [10.14336/AD.2024.0206](https://doi.org/10.14336/AD.2024.0206).
- [24] Jia Y, Qiu S, Xu J, et al. Exosomes secreted by young mesenchymal stem cells promote new bone formation during distraction osteogenesis in older rats[J]. Calcif Tissue Int, 2020, 106(5): 509-517. doi: [10.1007/s00223-019-00656-4](https://doi.org/10.1007/s00223-019-00656-4).
- [25] Weng Z, Wang Y, Ouchi T, et al. Mesenchymal stem/stromal cell senescence: hallmarks, mechanisms, and combating strategies[J]. Stem Cells Transl Med, 2022, 11(4): 356-371. doi: [10.1093/stcltm/szac004](https://doi.org/10.1093/stcltm/szac004).
- [26] Al-Azab M, Safi M, Idiattullina E, et al. Aging of mesenchymal stem cell: machinery, markers, and strategies of fighting[J]. Cell Mol Biol Lett, 2022, 27(1): 69. doi: [10.1186/s11658-022-00366-0](https://doi.org/10.1186/s11658-022-00366-0).
- [27] Cheng M, Yuan W, Moshaverinia A, et al. Rejuvenation of mesenchymal stem cells to ameliorate skeletal aging[J]. Cells, 2023, 12(7): 998. doi: [10.3390/cells12070998](https://doi.org/10.3390/cells12070998).
- [28] Melis S, Trompet D, Chagin AS, et al. Skeletal stem and progenitor cells in bone physiology, ageing and disease[J]. Nat Rev Endocrinol, 2025, 21(3): 135-153. doi: [10.1038/s41574-024-01039-y](https://doi.org/10.1038/s41574-024-01039-y).
- [29] Chen X, Luo Y, Zhu Q, et al. Small extracellular vesicles from young plasma reverse age-related functional declines by improving mitochondrial energy metabolism[J]. Nat Aging, 2024, 4(6): 814-838. doi: [10.1038/s43587-024-00612-4](https://doi.org/10.1038/s43587-024-00612-4).
- [30] Jiang X, Li W, Ge L, et al. Mesenchymal stem cell senescence during aging: from mechanisms to rejuvenation strategies[J]. Aging Dis, 2023, 14(5): 1651-1676. doi: [10.14336/AD.2023.0208](https://doi.org/10.14336/AD.2023.0208).

- [31] Li Y, Wu Q, Wang Y, et al. Senescence of mesenchymal stem cells (review) [J]. *Int J Mol Med*, 2017, 39(4): 775-782. doi: [10.3892/ijmm.2017.2912](https://doi.org/10.3892/ijmm.2017.2912).
- [32] Park SJ, Kim JM, Kim J, et al. Molecular mechanisms of biogenesis of apoptotic exosome-like vesicles and their roles as damage-associated molecular patterns[J]. *Proc Natl Acad Sci USA*, 2018, 115(50): e11721-e11730. doi: [10.1073/pnas.1811432115](https://doi.org/10.1073/pnas.1811432115).
- [33] Pavlyukov MS, Yu H, Bastola S, et al. Apoptotic cell-derived extracellular vesicles promote malignancy of glioblastoma *via* intercellular transfer of splicing factors[J]. *Cancer Cell*, 2018, 34(1): 119-135.e10. doi: [10.1016/j.ccell.2018.05.012](https://doi.org/10.1016/j.ccell.2018.05.012).
- [34] Gluchowska A, Cysewski D, Baj-Krzyworzeka M, et al. Unbiased proteomic analysis of extracellular vesicles secreted by senescent human vascular smooth muscle cells reveals their ability to modulate immune cell functions[J]. *Geroscience*, 2022, 44(6): 2863-2884. doi: [10.1007/s11357-022-00625-0](https://doi.org/10.1007/s11357-022-00625-0).
- [35] Boulestreau J, Maumus M, Bertolino Minani G, et al. Anti-aging effect of extracellular vesicles from mesenchymal stromal cells on senescence-induced chondrocytes in osteoarthritis[J]. *Aging (Albany NY)*, 2024, 16(21): 13252-13270. doi: [10.18632/aging.206158](https://doi.org/10.18632/aging.206158).
- [36] Zhang X, Tang J, Kou X, et al. Proteomic analysis of MSC-derived apoptotic vesicles identifies Fas inheritance to ameliorate haemophilia *a via* activating platelet functions[J]. *J Extracell Vesicles*, 2022, 11(7): e12240. doi: [10.1002/jev2.12240](https://doi.org/10.1002/jev2.12240).
- [37] Alsultan A, Farge D, Kili S, et al. International Society for Cell and Gene Therapy Clinical Translation Committee recommendations on mesenchymal stromal cells in graft-versus-host disease: easy manufacturing is faced with standardizing and commercialization challenges[J]. *Cytotherapy*, 2024, 26(10): 1132-1140. doi: [10.1016/j.jeyt.2024.05.007](https://doi.org/10.1016/j.jeyt.2024.05.007).
- [38] Adamo G, Picciotto S, Gargano P, et al. DetectEV: a functional enzymatic assay to assess integrity and bioactivity of extracellular vesicles[J]. *J Extracell Vesicles*, 2025, 14(1): e70030. doi: [10.1002/jev2.70030](https://doi.org/10.1002/jev2.70030).
- [39] Nguyen VVT, Witwer KW, Verhaar MC, et al. Functional assays to assess the therapeutic potential of extracellular vesicles[J]. *J Extracell Vesicles*, 2020, 10(1): e12033. doi: [10.1002/jev2.12033](https://doi.org/10.1002/jev2.12033).

(编辑 张琳)



Open Access

This article is licensed under a Creative Commons

Attribution 4.0 International License.

Copyright © 2026 by Editorial Department of Journal of Prevention and Treatment for Stomatological Diseases



官网